J. Fluid Mech. (2015), *vol.* 773, *pp.* 34–48.
doi:10.1017/jfm.2015.231

On the derivation of the HOMFLYPT polynomial invariant for fluid knots

Xin Liu[1] **and Renzo L. Ricca**[2,†]

[1]Beijing–Dublin International College and Institute of Theoretical Physics, Beijing University of Technology, 100 Pingleyuan, Beijing 100124, PR China

[2]Department of Mathematics and Applications, University of Milano-Bicocca, Via Cozzi 55, 20125 Milano, Italy

(Received 22 October 2014; revised 4 February 2015; accepted 17 April 2015)

By using and extending earlier results (Liu & Ricca, *J. Phys.* A, vol. 45, 2012, 205501), we derive the skein relations of the HOMFLYPT polynomial for ideal fluid knots from helicity, thus providing a rigorous proof that the HOMFLYPT polynomial is a new, powerful invariant of topological fluid mechanics. Since this invariant is a two-variable polynomial, the skein relations are derived from two independent equations expressed in terms of writhe and twist contributions. Writhe is given by addition/subtraction of imaginary local paths, and twist by Dehn's surgery. HOMFLYPT then becomes a function of knot topology and field strength. For illustration we derive explicit expressions for some elementary cases and apply these results to homogeneous vortex tangles. By examining some particular examples we show how numerical implementation of the HOMFLYPT polynomial can provide new insight into fluid-mechanical behaviour of real fluid flows.

Key words: mathematical foundations, topological fluid dynamics

1. Fluid knots and the Jones polynomial

In a series of papers (Liu & Ricca 2012, 2013) we have derived the skein relations of certain knot polynomials, such as the Kauffman bracket, the Alexander–Conway and the Jones polynomial, from the helicity of ideal fluid knots. Most notably, we have introduced the Jones polynomial as a new invariant of topological fluid mechanics (Ricca & Liu 2014). In the present paper, by relying on these earlier results we extend this approach further, and derive the HOMFLYPT polynomial (Freyd *et al.* 1985; Przytycki & Traczyk 1987), which is a two-variable version of the Jones polynomial. Since the HOMFLYPT skein relations are obtained by combining the independent contributions from writhe and twist helicity, we believe that HOMFLYPT provides a more powerful tool to detect topological complexity of fluid structures, such as vortex filaments in classical and quantized turbulence, and magnetic fields in astrophysical flows.

In the last couple of years striking evidence of the existence of knotted structures has been provided by a number of remarkable theoretical and experimental advances,

† Email address for correspondence: renzo.ricca@unimib.it

including the mathematical proof of the existence of knotted solutions to Euler equations (Enciso & Peralta-Salas 2012), the construction of knotted solutions to Maxwell equations (Kedia *et al.* 2013), and the laboratory production of vortex knots and links in water (Kleckner & Irvine 2013). Meanwhile, overwhelming evidence that vorticity and magnetic fields tend to self-organize into coherent flux tubes and bundles of filaments (Douady, Couder & Brachet 1991; Ishihara *et al.* 2007; Mouri, Hori & Kawashimab 2007; Baggaley *et al.* 2012; Cirtain *et al.* 2013), provides further evidence for possible new relationships between geometric and topological properties of complex fluid systems and energy contents (Barenghi, Ricca & Samuels 2001; Moisy & Jiménez 2004; Buck & Simon 2012; Ricca 2013; Kondaurova *et al.* 2014).

To investigate things further, and to fix ideas, let us consider a tangle of vortex filaments in an incompressible ideal fluid. Each vortex filament K (of small cross-section) is centred on a closed space curve X, of vector position $\boldsymbol{X}$. Vorticity is given by $\boldsymbol{\omega} = \boldsymbol{\nabla} \times \boldsymbol{u}$, where $\boldsymbol{u}$ is the associated velocity field. For a multi-component link $L = \cup_i K_i$ of N vortex filaments (possibly knotted), the helicity $H = H(L)$ is defined by

$$H(L) = \int_L \boldsymbol{u} \cdot \boldsymbol{\omega} \, \mathrm{d}^3\boldsymbol{x}, \tag{1.1}$$

where integration is done over the total volume of supp($\boldsymbol{\omega}$) in L. This is a well-known invariant of ideal fluid mechanics, that for thin filaments admits interpretation in terms of linking numbers (Moffatt 1969; Berger & Field 1984; Moffatt & Ricca 1992), i.e.

$$H = \sum_i SL_i \, \Phi_i^2 + 2 \sum_{i \neq j} Lk_{ij} \Phi_i \Phi_j, \tag{1.2}$$

where SL_i denotes the (Călugăreanu–White) self-linking number of X_i, Lk_{ij} is the (Gauss) linking number between X_i and X_j, and Φ_i is the ith flux (or circulation) of $\boldsymbol{\omega}$ within each K_i. For a single thin tubular knot in isolation, (1.1) takes the simple form

$$H(K) = \Phi \oint_K \boldsymbol{u} \cdot \mathrm{d}\boldsymbol{l}, \tag{1.3}$$

where $\boldsymbol{u}$ is the self-induced velocity given by the Biot–Savart law, and $\mathrm{d}\boldsymbol{l} \equiv \hat{\boldsymbol{t}} \, \mathrm{d}s$ the line element along the axis of K (where s is the arc-length and $\hat{\boldsymbol{t}}$ the unit tangent vector to X). By making use of a reference ribbon associated with the tubular knot, given by $R = R(\boldsymbol{X}, \hat{\boldsymbol{N}})$ (where $\hat{\boldsymbol{N}}$ is the unit normal vector to X), $H(K)$ admits decomposition in terms of writhe and twist, according to the Călugăreanu–White theorem (Moffatt & Ricca 1992; Ricca & Moffatt 1992):

$$H(K) = \Phi^2 SL = \Phi^2 (Wr + Tw), \tag{1.4}$$

where $Wr = Wr(X)$ is the writhing number of X, and $Tw = Tw(R)$ is the total twist number of R.

By analysing the knot properties in a standard knot diagram (see, for instance, Kauffman 1987), and by making use of a plausible statistical hypothesis on the state decomposition of the crossing sites (see Remark 3 at the end of § 3), Liu & Ricca (2012) (here below referred to as LR12) proved the following result.

THEOREM 1. *Let K denote a physical knot. If the helicity of K is $H = H(K)$, then*

$$\mathrm{e}^{H(K)} = \mathrm{e}^{\oint_K \boldsymbol{u} \cdot \mathrm{d}\boldsymbol{l}}, \tag{1.5}$$

appropriately re-scaled, satisfies (with a plausible statistical hypothesis) the skein relations of the Jones polynomial $V = V_K$.

Remark 1. To make sense of $e^{H(K)}$, $H(K)$ must be written in dimensionless form, by normalizing (1.3) with respect to some reference value of flux.

2. Kauffman's R polynomial and bracket polynomial

In general, a knot polynomial is generated by a set of rules, the so-called skein relations, that prescribe how a 'state' of a particular crossing site, represented for example by the over-crossing  in the knot diagram (see, for example, the leftmost diagram of figure 1), is related to its opposite (i.e. the under-crossing ) and the relative 'smoothing' given by two parallel strands (the non-crossing ). The recursive application of the skein relations to each crossing site allows the computation of the polynomial for a given knot (see the examples of § 4 below). In LR12, as a preliminary step towards the derivation of the Jones skein relations, we derived the skein relations of the so-called Kauffman R-polynomial for oriented knots (LR12, see equations (13)–(15)), given by

$$R\left(\;\right) = 1, \tag{2.1}$$

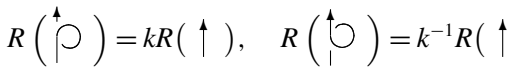

$$R\left(\;\right) = kR\left(\;\right), \quad R\left(\;\right) = k^{-1}R\left(\;\right), \tag{2.2a,b}$$

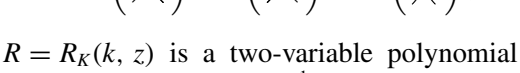

$$R\left(\;\right) - R\left(\;\right) = zR\left(\;\right), \tag{2.3}$$

where, in general, $R = R_K(k, z)$ is a two-variable polynomial of K in terms of the variables k and z. In LR12 we set $z = k - k^{-1}$, a choice instrumental for the derivation of the Jones polynomial $V = V_K(z)$, thus reducing R_K to the degenerate one-variable form known as the Alexander–Conway polynomial $\nabla = \nabla_K(z)$. In order to derive HOMFLYPT, that is, a two-variable polynomial $P = P_K(a, z)$, we must re-examine the derivation of (2.2) and introduce a second, independent relation for the variable a. By writing R in terms of $t^{H(K)}$ (where t is a dummy variable in the skein relation, and H is non-dimensional), and by using the virtual path decomposition shown in figure 1 for the positive figure-of-eight, we had

$$t^{H\left(\;\right)} = t^{H\left(\;\right)} t^{H\left(\;\right)} = t^{H\left(\;\right)} t^{H\left(\;\right)} = kt^{H\left(\;\right)}, \tag{2.4}$$

where by writing $H\left(\;\right) = H\left(\;\right)$ we implicitly assumed zero contribution from the helicity of the trivial circle, i.e. $t^{H\left(\;\right)} = 1$. A similar assumption made for the negative figure-of-eight led to

$$t^{H\left(\;\right)} = t^{H\left(\;\right)} t^{H\left(\;\right)} = t^{H\left(\;\right)} t^{H\left(\;\right)} = k^{-1}t^{H\left(\;\right)}. \tag{2.5}$$

Since R is the regular isotopy version of the HOMFLYPT polynomial, the necessary adjustment must be made by considering the writhe normalization of its regular isotopy counterpart (Kauffman 1987, 2001). On the other hand, physical insight for

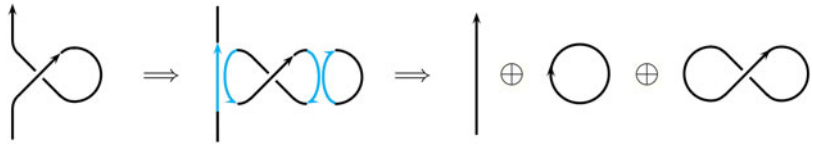

FIGURE 1. (Colour online) By virtually adding and subtracting local paths (denoted by blue arcs in the online version), a positive crossing can be reduced to a straight segment, a trivial circle and a (positive) figure-of-eight.

the appropriate correction comes from analysing the third skein relation of the bracket polynomial $B_K(\alpha) = \langle\cdot\rangle$ derived for unoriented knots (see LR12, equation (31)), given by

$$\left\langle \; \middle| \sqcup \bigcirc \right\rangle = f(\alpha)\left\langle \; \middle| \; \right\rangle, \tag{2.6}$$

where the presence of $f(\alpha)$, a function of the bracket variable α, suggests a possible contribution from the helicity associated with the circular loop (or any topologically equivalent configuration).

3. Derivation of the skein relations of the HOMFLYPT polynomial

Inspired by the helicity decomposition (1.4) in terms of writhe and twist, we can think of the skein relations as independent functions of the writhe and twist contribution, separately (see also Kauffman 2001, pp. 55–56). Hence, we propose to revise the derivation of the two skein relations for the HOMFLYPT polynomial $P = P_K(a, z)$ according to the following scheme.

(i) Skein relation for the z-variable: writhe contribution from crossing state information (regular isotopy).
(ii) Skein relation for the a-variable: twist contribution from Reidemeister type I move (ambient isotopy).

3.1. *Skein relation for the z-variable: writhe contribution*

Let us reconsider the Kauffman bracket skein relations for unoriented knots (LR12, equation (30)), given by

$$\left\langle \times \right\rangle = \alpha \left\langle \; \right\rangle \left\langle \; \right\rangle + \alpha^{-1} \left\langle \asymp \right\rangle, \tag{3.1}$$

$$\left\langle \times \right\rangle = \alpha \left\langle \asymp \right\rangle + \alpha^{-1} \left\langle \; \right\rangle \left\langle \; \right\rangle. \tag{3.2}$$

Here $\alpha = t^{\lambda_1 H(\bigcirc\bigcirc)}$ arises from the technique of adding/subtracting imaginary paths (as in figure 1; see also LR12, figure 6), and λ_1 is a parameter that takes into account the uncertainty associated with the writhe value of $\bigcirc\bigcirc$. By endowing the knot strands in (3.1) and (3.2) with orientation, we have

$$\left\langle \times \right\rangle = \alpha \left\langle \; \right\rangle \left\langle \; \right\rangle + \alpha^{-1} \left\langle \asymp \right\rangle, \tag{3.3}$$

$$\left\langle \times \right\rangle = \alpha \left\langle \asymp \right\rangle + \alpha^{-1} \left\langle \; \right\rangle \left\langle \; \right\rangle. \tag{3.4}$$

The (inconsistent) term $\langle$  $\rangle$ on the right-hand side of the above equations vanishes by considering the difference between crossing states, that is,

$$\alpha \left\langle \right\rangle - \alpha^{-1} \left\langle \right\rangle = (\alpha^2 - \alpha^{-2}) \left\langle \right\rangle . \tag{3.5}$$

The R-polynomial of a knot K is readily obtained from its bracket polynomial $\langle\cdot\rangle$ by the standard position (Kauffman 2001)

$$R[K] = \alpha^w \langle K \rangle, \tag{3.6}$$

where w is the (directional) writhe of the knot diagram $[K]$. By applying (3.6) to a non-crossing state of $[K]$, we have

$$R \left(\right) = \alpha^w \left\langle \right\rangle . \tag{3.7}$$

By switching the non-crossing state to an over-crossing (or an under-crossing), and by applying (3.6), we have

$$R \left(\right) = \alpha^{w+1} \left\langle \right\rangle , \quad R \left(\right) = \alpha^{w-1} \left\langle \right\rangle . \tag{3.8a,b}$$

Hence, by taking the difference between the two states, and by using (3.7), we have

$$\begin{aligned} R \left(\right) - R \left(\right) &= \alpha^w \left(\alpha \left\langle \right\rangle - \alpha^{-1} \left\langle \right\rangle \right) \\ &= (\alpha^2 - \alpha^{-2}) \alpha^w \left\langle \right\rangle = (\alpha^2 - \alpha^{-2}) R \left(\right) . \end{aligned} \tag{3.9}$$

By defining $k = \alpha^2$ and $z = k - k^{-1}$, one of the skein relations of the R polynomial is readily obtained:

$$R \left(\right) - R \left(\right) = z R \left(\right) . \tag{3.10}$$

The skein relation for the z-variable of the HOMFLYPT polynomial is finally derived by the standard position (Kauffman 2001, pp. 650–651)

$$P(a, z) = a^{-w} R(a, z), \tag{3.11}$$

where a will be defined in terms of twist in the following subsection (see (3.17) below). Since

$$w \left[\right] = +1, \quad w \left[\right] = -1, \tag{3.12a,b}$$

and

$$w \left[\right] = w \left[\right] = w \left[\right] = 0, \tag{3.13}$$

we have

$$aP \left(\right) - a^{-1} P \left(\right) = z P \left(\right) . \tag{3.14}$$

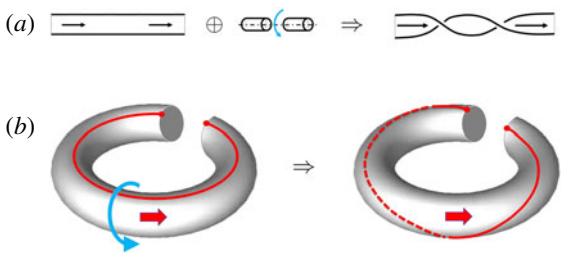

FIGURE 2. (Colour online) (*a*) By using a reference ribbon, twist can be visualized by a local insertion on the straight band. (*b*) Twist insertion by Dehn surgery on a torus.

3.2. *Skein relation for the a-variable: twist contribution*

As discussed in earlier works (Moffatt 1990; Ricca & Moffatt 1992), twist insertion by Dehn surgery (see, for example, Adams 1999) provides an idealized technique for twist insertion in fluid knots; by using the reference ribbon concept (see figure 2), twist insertion can be realized by a three-step mathematical process given by a virtual cut, rotation and reconnection (in this sequence) performed locally on the knot strand. By using the standard decomposition of helicity in terms of writhe and twist (see (1.4)), Dehn surgery can thus be interpreted as a technique for insertion/deletion of (twist) helicity alternative (and complementary) to the insertion/deletion of helicity provided by the virtual addition/subtraction of imaginary local paths through a change of writhe (as in figure 1).

By using the ribbon representation of knot strands, we replace the idealized scheme of figure 1 with that of figure 3. Thus, twist insertion/deletion in the unknotted ribbon  gives  , and contributes to twist helicity, according to the decomposition

$$\tau = H\left(\quad\right) = H\left(\quad\right) + H\left(\quad\right); \tag{3.15}$$

Hence, we can replace (2.4) and (2.5) with

$$t^{H}\left(\quad\right) = t^{H}\left(\quad\right) t^{H}\left(\quad\right) t^{H}\left(\quad\right) = a t^{H}\left(\quad\right), \tag{3.16}$$

$$t^{H}\left(\quad\right) = t^{H}\left(\quad\right) t^{H}\left(\quad\right) t^{H}\left(\quad\right) = a^{-1} t^{H}\left(\quad\right), \tag{3.17}$$

where $a = t^{\tau}$. Thus (2.2) are replaced by

$$R\left(\quad\right) = aR\left(\quad\right), \quad R\left(\quad\right) = a^{-1}R\left(\quad\right); \tag{3.18a,b}$$

Using (3.11), these correspond to

$$P\left(\quad\right) = P\left(\quad\right), \quad P\left(\quad\right) = P\left(\quad\right). \tag{3.19a,b}$$

Following LR12, and by using the same change of variables introduced by Liu & Ricca (2013) (by taking $t = e$), without loss of generality we can set

$$\left.\begin{array}{ll} k = \alpha^2 = \mathrm{e}^{\bar{\omega}}, & \bar{\omega} = 2\lambda_{\omega} H\left(\quad\right) \\ a = \mathrm{e}^{\bar{\tau}}, & \bar{\tau} = \lambda_{\tau} H\left(\quad\right) \end{array}\right\} \quad \{\lambda_{\omega}, \lambda_{\tau}\} \in [0, 1], \tag{3.20}$$

FIGURE 3. (Colour online) By using a ribbon representation of knot strands, a (positive) crossing can be virtually decomposed into a straight ribbon and a circular band with (positive) twist.

where λ_ω and λ_τ are two parameters that take into account the uncertainty (or probability) associated with writhe and twist values of some reference configuration (as in figure 7 of LR12).

The skein relations of the HOMFLYPT polynomial for oriented knots are given by (2.1) and (3.14):

$$P\left(\bigcirc\right) = 1, \tag{3.21}$$

$$aP\left(\times\right) - a^{-1}P\left(\times\right) = zP\left(\rightleftharpoons\right), \tag{3.22}$$

where $z = k - k^{-1}$. Thus, we have proved the following result.

THEOREM 2. *Let K denote a physical knot. If the helicity of K is $H = H(K)$, then*

$$\mathrm{e}^{H(K)} = \mathrm{e}^{\oint_K \boldsymbol{u}\cdot\mathrm{d}\boldsymbol{l}}, \tag{3.23}$$

appropriately re-scaled, satisfies (with a plausible statistical hypothesis) the skein relations of the HOMFLYPT polynomial $P = P_K$.

Remark 2. To make sense of $\mathrm{e}^{H(K)}$, $H(K)$ must be written in dimensionless form, by normalizing (1.3) with respect to some reference value of the field strength.

Remark 3. The derivation of the result above relies on the following statistical hypothesis (instrumental for the derivation of the Kauffman bracket polynomial and the skein relation for the z-variable in § 3.1; see LR12, section 4.1): the contribution of the unoriented crossing to the skein relation is computed by assuming a virtual branching process of the crossing, which leads to two independent, equally probable states (represented by the left–right and up–down schemes shown in figure 4). In the absence of specific prescriptions, this is equivalent to the ergodic assumption that all possible (virtual) reconfiguration states of the given knot or link are admissible and equally probable. Particular fluid-mechanical specifications, suggested by the physics of the process, will eventually help to select specific conditions for the most appropriate statistics.

The skein relations (3.21) and (3.22) generate the HOMFLYPT polynomial $P = P_K$. For a link of N components, since each knot carries information about its own field strength, and $H(K)$ is a diffeomorphic invariant of K, then P_K is a diffeomorphic invariant of knot type and flux. Hence, we have the following corollary.

COROLLARY 1. *The HOMFLYPT polynomial provides a new invariant of ideal fluid mechanics, by extending the dual dependence of helicity on linking number and flux.*

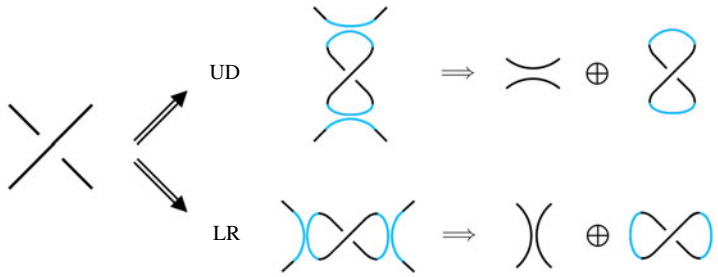

FIGURE 4. (Colour online) The unoriented crossing on the left can be virtually split by adding and subtracting local paths (denoted by blue arcs in the online version) following the up–down (UD) or the left–right (LR) scheme above. Both decompositions are assumed to contribute equally to the computation in the skein relation.

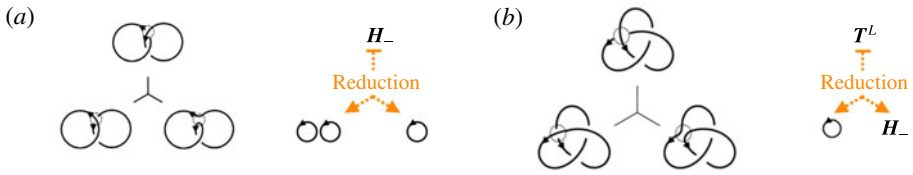

FIGURE 5. (Colour online) Reduction schemes for the Hopf link $\boldsymbol{H}_-$ and the trefoil knot $\boldsymbol{T}^L$.

4. HOMFLYPT polynomial of some elementary cases

For the purpose of illustration we present explicit calculations of the HOMFLYPT polynomial of some elementary cases. HOMFLYPT polynomials of more complex topologies can be readily computed by some of the knot tabulators available online (such as KnotAtlas). Implementation of the HOMFLYPT skein relations rely on reduction schemes exemplified by the diagrams of figure 5. As well as their mathematical meaning, these diagrams acquire physical significance when the fluid evolution is governed by reduction in topological complexity based on single reconnection events (as discussed in the second example of § 6). As we shall see, reduction schemes can also provide physical intuition for realistic cascade processes in turbulent flows.

4.1. *N disjoint, unknotted loops* $\boldsymbol{U}_N$

For a single loop the initial condition of the skein relations (3.21) prescribes $P(\bigcirc) = P(\bigcirc\!\!\bigcirc) = P(\bigcirc\!\!\bigcirc) = 1$; this can be used to determine the polynomial of two unknotted loops $\boldsymbol{U}_2$. By using (3.22), we have

$$aP(\bigcirc\!\!\bigcirc) - a^{-1}P(\bigcirc\!\!\bigcirc) = zP\left(\bigcirc\ \bigcirc\right); \tag{4.1}$$

Hence

$$P(\boldsymbol{U}_2) = P\left(\bigcirc\ \bigcirc\right) = P(\bigcirc)\frac{a-a^{-1}}{z} = \frac{a-a^{-1}}{k-k^{-1}} = \delta. \tag{4.2}$$

Similarly for three unknotted loops $\boldsymbol{U}_3$, by (3.22), we have

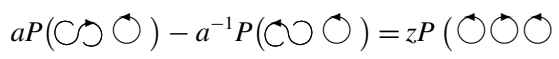

$$aP(\quad) - a^{-1}P(\quad) = zP(\quad), \tag{4.3}$$

so that

$$P(\boldsymbol{U}_3) = P(\quad)\frac{a-a^{-1}}{z} = \left[\frac{a-a^{-1}}{k-k^{-1}}\right]^2 = \delta^2. \tag{4.4}$$

In general, for a disjoint union of N oriented, unknotted loops $\boldsymbol{U}_N$, we have

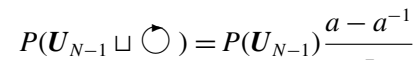

$$P(\boldsymbol{U}_{N-1} \sqcup \quad) = P(\boldsymbol{U}_{N-1})\frac{a-a^{-1}}{z}; \tag{4.5}$$

Hence

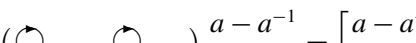

$$P(\boldsymbol{U}_N) = P(\quad)\frac{a-a^{-1}}{z} = \left[\frac{a-a^{-1}}{k-k^{-1}}\right]^{N-1} = \delta^{N-1}. \tag{4.6}$$

Note that in this case the value of the polynomial does not depend on the relative orientation of the loops.

4.2. *Hopf link*

For the negative Hopf link $\boldsymbol{H}_-$ (see figure 5*a*), we have

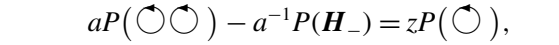

$$aP(\quad) - a^{-1}P(\boldsymbol{H}_-) = zP(\quad), \tag{4.7}$$

so that

$$P(\boldsymbol{H}_-) = a^3z^{-1} - az^{-1} - az. \tag{4.8}$$

4.3. *Left-handed trefoil knot*

For the left-handed trefoil knot $\boldsymbol{T}^L$ (see figure 5*b*), we have

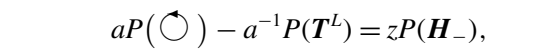

$$aP(\quad) - a^{-1}P(\boldsymbol{T}^L) = zP(\boldsymbol{H}_-), \tag{4.9}$$

so that

$$P(\boldsymbol{T}^L) = 2a^2 + a^2z^2 - a^4. \tag{4.10}$$

5. Quantifying structural complexity by topological information

In this section we present the HOMFLYPT computation of some simple topological cases, highlighting some key features relevant to fluid systems. From a physical viewpoint the HOMFLYPT polynomial $P = P_K(a, z)$ is not only a new invariant of topological fluid mechanics, but it can take into account the contributions from writhe and twist separately, through the z and a variables. From this viewpoint it appears to be more powerful than the Jones (and Alexander–Conway) polynomial. Indeed, HOMFLYPT reduces to Jones when we take $a = \tau^{-1}$ and $k = \tau^{1/2}$ (see LR12, equation (37)); thus, by (3.20), we have

$$ak^2 = \mathrm{e}^{\bar{\tau}}\mathrm{e}^{2\bar{\omega}} = 1, \tag{5.1}$$

Knot type	HOMFLYPT polynomial	Numerical value
$\boldsymbol{U}_N$	$\delta^{N-1} = [(a - a^{-1})z^{-1}]^{N-1}$	0.48^{N-1}
$\boldsymbol{H}_+$	$a^{-1}z + (a^{-1} - a^{-3})z^{-1}$	1.10
$\boldsymbol{H}_-$	$-az - (a - a^3)z^{-1}$	–0.54
$\boldsymbol{T}^L$	$2a^2 + a^2z^2 - a^4$	2.36
$\boldsymbol{T}^R$	$2a^{-2} + a^{-2}z^2 - a^{-4}$	1.51
$\boldsymbol{F}^8$	$a^{-2} - 1 - z^2 + a^2$	0.17
$\boldsymbol{W}$	$-a^{-1}z^{-1} - a^{-1}z + az^{-1} + 2az + az^3 - a^3z$	1.59
$\tilde{\boldsymbol{W}}$	$az^{-1} + az - a^{-1}z^{-1} - 2a^{-1}z - a^{-1}z^3 + a^{-3}z$	–0.20
$\boldsymbol{B}$	$a^{-2}z^{-2} - a^{-2}z^2 + a^2z^{-2} - a^2z^2 - 2z^{-2} + 2z^2 + z^4$	1.13

FIGURE 6. Numerical values of the HOMFLYPT polynomial of some elementary knots and links for $\Phi = 1$, $k = \mathrm{e}^{1/2}$, $a = \mathrm{e}^{1/4}$, $z = k - k^{-1}$. $\boldsymbol{U}_N$ denotes $N > 1$ disjoint unlinked, unknotted loops, $\boldsymbol{H}_+$ the positive Hopf link, $\boldsymbol{H}_-$ the negative Hopf link, $\boldsymbol{T}^L$ the left-hand trefoil, $\boldsymbol{T}^R$ the right-hand trefoil, $\boldsymbol{F}^8$ the figure-of-eight knot, $\boldsymbol{W}$ the Whitehead link, $\tilde{\boldsymbol{W}}$ the mirror image of the Whitehead link, and $\boldsymbol{B}$ the Borromean rings.

that is,

$$\lambda_\tau Tw = -4\lambda_\omega Wr, \tag{5.2}$$

which poses a rather strict constraint on the admissible writhe and twist contributions of the reference mean flow field. We point out that this constraint is absent in the case of HOMFLYPT, where writhe and twist can indeed take any possible real value independently.

For simplicity let us set $\Phi = 1$ for all knot types (as in the case of superfluid vortex tangles). The values of$H(\bigcirc\!\!\circlearrowright) = Wr$ and $H\big(\circlearrowleft\!\!\bigcirc\big) = Tw$ can be either derived from global helicity measurements based on (1.1), or estimated on the basis of computational/observational data of the flow field (see, for example, Barenghi *et al.* 2001). Writhe can be directly computed from geometric analysis of the tangle, whereas twist can be obtained as the difference between helicity, given by (1.1), and the sum of (Gauss) linking numbers and writhe, by using (1.2). Hence, the vortex tangle will be identified by HOMFLYPT information (implemented by numerical codes in real-time analysis) computed on the basis of the mean flow field values given by $\langle Wr \rangle$ and $\langle Tw \rangle$ (and mirror contributions). In the absence of such information (and here for the sake of illustration) we take

$$\langle Wr \rangle = \tfrac{1}{2}, \quad \lambda_\omega = \tfrac{1}{2} \Rightarrow k = \mathrm{e}^{1/2}, \tag{5.3}$$

$$\langle Tw \rangle = \tfrac{1}{2}, \quad \lambda_\tau = \tfrac{1}{2} \Rightarrow a = \mathrm{e}^{1/4}. \tag{5.4}$$

Let us consider the following cases: N disjoint unlinked, unknotted loops $\boldsymbol{U}_N$, the positive Hopf link $\boldsymbol{H}_+$, the negative Hopf link $\boldsymbol{H}_-$, the left-hand trefoil $\boldsymbol{T}^L$, the right-hand trefoil $\boldsymbol{T}^R$, the figure-of-eight knot $\boldsymbol{F}^8$, the Whitehead link $\boldsymbol{W}$, the mirror image of the Whitehead link $\tilde{\boldsymbol{W}}$, and the Borromean rings $\boldsymbol{B}$. The corresponding polynomial expressions and their numerical values are shown in the table of figure 6.

Since individual loops are frequently formed in fluid dynamical systems (as a result of physical interaction and reconnection), the case of unlinked, unknotted loops

deserves particular interest. From (3.20) and (4.1), we have

$$\delta = \frac{a - a^{-1}}{k - k^{-1}} = \frac{\mathrm{e}^{\bar{\tau}} - \mathrm{e}^{-\bar{\tau}}}{\mathrm{e}^{\bar{\omega}} - \mathrm{e}^{-\bar{\omega}}} = \frac{\sinh \bar{\tau}}{\sinh \bar{\omega}}, \tag{5.5}$$

with $\delta \to \bar{\tau}/\bar{\omega}$ when both $\bar{\tau}$ and $\bar{\omega}$ tend to 0.

In practice, the precise value of a, a^{-1}, k and k^{-1} depend on the particular physical context, and marked differences are indeed possible (for instance between vortex and magnetic systems), particularly so as regards the value of a and a^{-1}. For vortex flows, twist is expected to be consistent with the tube vorticity direction and orientation, and so mainly positive. This means that the probability of having a and a^{-1} values equi-distributed is very low; hence, a and a^{-1} should be weighted by numerically different values, say λ_{τ^+} and λ_{τ^-}, with $0 \leqslant \lambda_{\tau^-} \ll \lambda_{\tau^+} \leqslant 1$. This is not the case for magnetic flux tubes in astrophysical flows, where twist (often of mechanical origin) is not explicitly related to the magnetic field direction (although the polarities of vortical regions are often correlated). There are also physical limits to twist values related to writhe or kink instabilities, for which $Tw = O(1)$. Writhe, on the other hand, does not suffer from such limitations, with no particular constraints on λ_{ω^+} and λ_{ω^-}.

Finally, we would like to mention a remarkable property of HOMFLYPT, which can be exploited by numerical implementation of structural complexity methods. This is summarized by the following set of rules (Lickorish & Millett 1988).

PROPOSITION 1.

$$P(L_1 \# L_2) = P(L_1)P(L_2); \tag{5.6}$$

$$P(L_1 \sqcup L_2) = \delta P(L_1)P(L_2). \tag{5.7}$$

In (5.6) $L_1 \# L_2$ denotes the connected sum of any component of the oriented link L_1 with any component of the oriented link L_2; in (5.7) $L_1 \sqcup L_2$ denotes the disjoint union of L_1 and L_2, assuming that L_1 and L_2 are placed at some distance apart, so that no part of L_1 crosses over or under any part of L_2. Note that direct application of (5.7) to the case of N disjoint loops gives (4.6).

6. New insight into fluid-mechanical behaviour

Numerical implementation of HOMFLYPT provides useful information to gain new insight into fluid-mechanical behaviour of real fluid flows. Here we mention some possible applications that we believe will be helpful for turbulence research.

(i) As experiments and direct numerical simulations of superfluid turbulence show (Tsubota, Araki & Nemirovskii 2000; Leadbeater *et al.* 2003; Kondaurova *et al.* 2014), vortex tangles evolve through continuous production and interaction of small(er)-scale unlinked, unknotted vortex loops. Evidence shows that these loops are planar ring-like structures, with almost no writhe and no twist (superfluid vortices are like empty tubes with no internal structure); thus, their internal helicity is either zero or negligible. Being unlinked to the rest of the system, these loops do not contribute to the total helicity of the system; thus, as far as helicity is concerned, they are like ghost structures. In terms of energy, though, their contribution is not negligible, since they interact dynamically with the rest of the system. Hence, any information on the relationship between helicity, taken as a measure of structural complexity, and energy cannot be accurate enough. Moreover, in cases such as those exemplified by the Whitehead link or the Borromean rings, where the linking number fails to distinguish

essential links from unlinked systems, this information gives completely incorrect results. From this viewpoint HOMFLYPT provides not only a more accurate account of the topological complexity of the flow, but it can also distinguish situations where a given number of loops are present (see § 4.1): indeed, being $P(\boldsymbol{U}_N)$ invertible, it can be used to track the precise number N of unlinked, unknotted vortex rings present in the fluid. This information, related to energy, can help to establish detailed relationships between topological complexity and energy.

(ii) The recent laboratory experiments on the production and free decay of vortex knots and links in water (Kleckner & Irvine 2013) show that both trefoil knots and Hopf links follow a similar reconnection cascade: the topology gets gradually reduced, with complexity reduced in steps of one crossing lost at each reconnection event, until final dissipation of unlinked, unknotted smaller loops. Remarkably, a similar reconnection pattern (which brings the trefoil knot to the Hopf link, the unknot and the unlink of two smaller unknotted loops) is also shown to characterize DNA recombination: quite remarkably, a mathematically rigorous characterization of the topological mechanism of DNA unlinking is shown to be the only possible pathway that strictly reduces complexity by stepwise unlinking (Shimokawa *et al.* 2013). The mathematics behind this proof suggests that it would be equally applicable to flux tube reconnections. In any case, if the change in topology is due to a single reconnection event, the reconnection pattern can be reproduced by following the 'smoothing' sequence of the reduction scheme shown in § 4. For example, by combining the schemes of figure 5(*b*,*a*) (in this order), we have

$$\boldsymbol{T}^L \rightsquigarrow \boldsymbol{H}_- \rightsquigarrow \boldsymbol{U}_1 \rightsquigarrow \boldsymbol{U}_2, \tag{6.1}$$

where the last step is due to the application of the skein relation to the coiled unknot (because of the presence of the apparent crossing) to produce two smaller rings. By analysing the smoothing process of more complex topologies we can make predictions of typical reconnection cascades. For the Borromean rings, for example, a simple exercise shows that we should expect something like

$$\boldsymbol{B} \rightsquigarrow \tilde{\boldsymbol{W}} \rightsquigarrow \boldsymbol{T}^R \rightsquigarrow \boldsymbol{H}_+ \rightsquigarrow \boldsymbol{U}_1 \rightsquigarrow \boldsymbol{U}_2, \tag{6.2}$$

or

$$\boldsymbol{B} \rightsquigarrow \boldsymbol{W} \rightsquigarrow \boldsymbol{F}^8 \rightsquigarrow \boldsymbol{H}_- \rightsquigarrow \boldsymbol{U}_1 \rightsquigarrow \boldsymbol{U}_2, \tag{6.3}$$

according to whether the first reconnection event takes place in the outer or inner region of $\boldsymbol{B}$. Numerical implementation of these ideas to analyse more complex situations will provide information on preferential decay patterns for structural complexity and energy.

(iii) Direct numerical implementation of software dedicated to topological analysis of fluid structures is readily available. Rob Scharein's KnotPlot, for example, can analyse data extracted from fluid flow simulations (by tracking vorticity, magnetic field, low pressure, or density regions), and compute the HOMFLYPT polynomial to any degree of accuracy. Similar analyses made on complex tangles of superfluid vortices (Barenghi *et al.* 2001; Kondaurova *et al.* 2014) proved that this can be done rather efficiently. By relating changes in topology and structural complexity to changes in energy, this process can be iterated in real time, so as to have a time-dependent information on adaptive topology by HOMFLYPT implementation. This approach can be used to reveal the presence of hierarchical order, occurrence of generic reconnection pathways and preferential routes to energy dissipation.

7. Conclusions

In this paper we provide a rigorous proof of the derivation of the HOMFLYPT polynomial invariant from the helicity of fluid knots and links (Theorem 2), by deriving the HOMFLYPT skein relations from helicity (§§ 3.1 and 3.2). Since in ideal conditions vortex (or magnetic) lines are transported, with constant flux, by the flow of an ideal fluid, their topology is conserved in time. Hence, our result establishes HOMFLYPT as a new invariant of topological fluid mechanics (Corollary 1). Proof of the derivation of the HOMFLYPT skein relations for the variables a and z necessary for the polynomial computation is done in two steps: in § 3.1, by interpreting the contribution in the z variable in terms of writhe, and in § 3.2, by relating a to the twist contribution. The physical interpretation of the skein relations in terms of writhe and twist contributions appears to be new and illuminates the respective role of the skein relation in the HOMFLYPT computation. As illustration, a number of simple cases are considered (§ 4), including the case of a system of N disjoint, unknotted loops, the Hopf link and the left-handed trefoil knot, all typical examples of topological structures that are likely to occur in real fluid flows. Moreover, the reduction schemes associated with the skein relations (as shown in the examples of figure 5) seem to provide useful physical intuition for typical reconnection cascade patterns, when topological complexity gets reduced by a single reconnection event. In § 5 we apply HOMFLYPT to the case of a homogeneous tangle of vortex filaments of equal circulation, and we compute numerical values for a number of cases, including the Whitehead link and the Borromean rings, both having linking number zero. Real-time, direct numerical implementation of HOMFLYPT will provide useful information to gain new insight into fluid-mechanical behaviour of real fluid flows. In § 6 we give three examples: (i) the HOMFLYPT ability to detect the presence of zero-linking number structures (such as a system of unlinked vortex rings), that otherwise would escape the helicity count; (ii) the prediction of typical reconnection cascade patterns for structures that evolve by reducing complexity through a single reconnection event, by using the reduction schemes associated with the polynomial skein relations; (iii) the HOMFLYPT flow data analysis by dedicated software (such as KnotPlot) to establish time-dependent relationships between structural complexity, energy transfers and dissipation rates. Implementation of HOMFLYPT as a new diagnostic tool in direct numerical simulations of classical and superfluid turbulent flows might prove useful in determining new connections between energy localization and transfer.

Acknowledgements

We wish to thank the Isaac Newton Institute for Mathematical Sciences for the kind hospitality and support provided during our stay in Cambridge (UK), where part of this work was initiated. We would also like to thank Ken Millett for his comments on a preliminary version of this paper.

REFERENCES

ADAMS, C. 1999 *The Knot Book*. Freeman.

BAGGALEY, A. W., BARENGHI, C. F., SHUKUROV, A. & SERGEEV, Y. A. 2012 Coherent vortex structures in quantum turbulence. *Europhys. Lett.* **98**, 26002.

BARENGHI, C. F., RICCA, R. L. & SAMUELS, D. C. 2001 How tangled is a tangle? *Physica* D **157**, 197–206.

BERGER, M. A. & FIELD, G. B. 1984 The topological properties of magnetic helicity. *J. Fluid Mech.* **147**, 133–148.

BUCK, S. & SIMON, J. 2012 The spectrum of filament entanglement complexity and an entanglement phase transition. *Proc. R. Soc. Lond.* A **468**, 4024–4040.

CĂLUGĂREANU, G. 1961 Sur les classes d'isotopie des nœuds tridimensionnels et leurs invariants. *Czechoslovak Math. J.* **11**, 588–625.

CIRTAIN, J. W., GOLUB, L., WINEBARGER, A. R., DE PONTIEU, B., KOBAYASHI, K., MOORE, R. L., WALSH, R. W., KORRECK, K. E., WEBER, M., MCCAULEY, P., TITLE, A., KUZIN, S. & DEFOREST, C. E. 2013 Energy release in the solar corona from spatially resolved magnetic braids. *Nature* **493**, 501–503.

DOUADY, S., COUDER, Y. & BRACHET, M. E. 1991 Direct observation of the intermittency of intense vorticity filaments in turbulence. *Phys. Rev. Lett.* **67**, 983–986.

ENCISO, A. & PERALTA-SALAS, D. 2012 Knots and links in steady solutions of the Euler equation. *Ann. Maths* **175**, 345–367.

FREYD, P., YETTER, D., HOSTE, J., LICKORISH, W. B. R., MILLETT, K. & OCNEANU, A. 1985 A new polynomial invariant of knots and links. *Bull. Am. Math. Soc.* **12**, 239–246.

ISHIHARA, T., KANEDA, Y., YOKOKAWA, M., ITAKURA, K. & UNO, A. 2007 Small-scale statistics in high-resolution direct numerical simulation of turbulence: Reynolds number dependence of one-point velocity gradient statistics. *J. Fluid Mech.* **592**, 335–366.

KAUFFMAN, L. H. 1987 *On Knots*. Princeton University Press.

KAUFFMAN, L. H. 2001 *Knots and Physics*. World Scientific.

KEDIA, H., BIALYNICKI-BIRULA, I., PERALTA-SALAS, D. & IRVINE, W. T. M. 2013 Tying knots in light fields. *Phys. Rev. Lett.* **111**, 150404.

KLECKNER, D. & IRVINE, W. T. M. 2013 Creation and dynamics of knotted vortices. *Nat. Phys.* **9**, 253–258.

KnotAtlas: http://katlas.math.toronto.edu/wiki/Main_Page.

KnotPlot: http://www.knotplot.com.

KONDAUROVA, L., L'VOV, V., POMYALOV, A. & PROCACCIA, I. 2014 Structure of quantum vortex tangle in ^{4}He counterflow turbulence. *Phys. Rev.* B **89**, 014502.

LEADBEATER, M., SAMUELS, D. C., BARENGHI, C. F. & ADAMS, C. S. 2003 Decay of superfluid turbulence via Kelvin-wave radiation. *Phys. Rev.* A **67**, 015601.

LICKORISH, W. B. R. & MILLETT, K. C. 1988 The new polynomial invariants of knots and links. *Maths Mag.* **61**, 3–23.

LIU, X. & RICCA, R. L. 2012 The Jones polynomial for fluid knots from helicity. *J. Phys.* A **45**, 205501.

LIU, X. & RICCA, R. L. 2013 Tackling fluid structures complexity by the Jones polynomial. In *Topological Fluid Dynamics: Theory and Applications* (ed. H. K. Moffatt, K. Bajer & Y. Kimura), Procedia IUTAM, vol. 7, pp. 175–182. Elsevier.

MOFFATT, H. K. 1969 The degree of knottedness of tangled vortex lines. *J. Fluid Mech.* **35**, 117–129.

MOFFATT, H. K. 1990 The energy spectrum of knots and links. *Nature* **347**, 367–369.

MOFFATT, H. K. & RICCA, R. L. 1992 Helicity and the Călugăreanu invariant. *Proc. R. Soc. Lond.* A **439**, 411–429.

MOISY, F. & JIMÉNEZ, J. 2004 Geometry and clustering of intense structures in isotropic turbulence. *J. Fluid Mech.* **513**, 111–133.

MOURI, H., HORI, A. & KAWASHIMAB, Y. 2007 Laboratory experiments for intense vortical structures in turbulence velocity fields. *Phys. Fluids* **19**, 055101.

PRZYTYCKI, J. H. & TRACZYK, P. 1987 Conway algebras and skein equivalence of links. *Proc. Am. Math. Soc.* **100**, 744–748.

RICCA, R. L. 2013 New energy and helicity lower bounds for knotted and braided magnetic fields. *Geophys. Astrophys. Fluid Dyn.* **107**, 385–402.

RICCA, R. L. 2014 Structural complexity of vortex flows by diagram analysis and knot polynomials. In *How Nature Works* (ed. I. Zelinka, A. Sanayei, H. Zenil & O. E. Rössler), Emergence, Complexity and Computation, vol. 5, pp. 81–100. Springer.

RICCA, R. L. & LIU, X. 2014 The Jones polynomial as a new invariant of topological fluid dynamics. *Fluid Dyn. Res.* **46**, 061412.

RICCA, R. L. & MOFFATT, H. K. 1992 The helicity of a knotted vortex filament. In *Topological Aspects of the Dynamics of Fluids and Plasmas* (ed. H. K. Moffatt, G. M. Zaslavsky, P. Comte & M. Tabor), pp. 225–236. Kluwer Academic.

SHIMOKAWA, K., ISHIHARA, K., GRAINGE, I., SHERRATT, D. J. & VAZQUEZ, M. 2013 FtsK-dependent XerCD-*dif* recombination unlinks replication catenanes in a stepwise manner. *Proc. Natl Acad. Sci. USA* **110**, 20906–20911.

TSUBOTA, M., ARAKI, T. & NEMIROVSKII, S. K. 2000 Dynamics of vortex tangle without mutual friction in superfluid ^{4}He. *Phys. Rev.* B **62**, 11751–11762.